Registration performance on EUV masks using high-resolution registration metrology

Steffen Steinert[a], Hans-Michael Solowan[a], Jinback Park[b], Hakseung Han[b], Dirk Beyer[a], Thomas Scherübl[a]

[a]Carl Zeiss SMT, ZEISS Group, Carl-Zeiss-Promenade 10, 07745 Jena
[b]Samsung, Mask Development Team, San #16 Banwol-Dong, Hwasung-City

ABSTRACT

Next-generation lithography based on EUV continues to move forward to high-volume manufacturing. Given the technical challenges and the throughput concerns a hybrid approach with 193 nm immersion lithography is expected, at least in the initial state. Due to the increasing complexity at smaller nodes a multitude of different masks, both DUV (193 nm) and EUV (13.5 nm) reticles, will then be required in the lithography process-flow. The individual registration of each mask and the resulting overlay error are of crucial importance in order to ensure proper functionality of the chips. While registration and overlay metrology on DUV masks has been the standard for decades, this has yet to be demonstrated on EUV masks. Past generations of mask registration tools were not necessarily limited in their tool stability, but in their resolution capabilities. The scope of this work is an image placement investigation of high-end EUV masks together with a registration and resolution performance qualification. For this we employ a new generation registration metrology system embedded in a production environment for full-spec EUV masks. This paper presents excellent registration performance not only on standard overlay markers but also on more sophisticated e-beam calibration patterns.

Key words: Registration, Photomask, PROVE®, Overlay, Double Patterning, Image Placement, EUV

INTRODUCTION

The extension of optical lithography operating at 193 nm illumination wavelength down to the 10 nm node and below has increased the complexity and production costs significantly. Although still facing multiple challenges such as source power and blank defectivity [1], EUV is nevertheless widely accepted as future technology to meet the semiconductor industry's need beyond the 10 nm node. The introduction of EUV technology into production is currently targeted for the 7 nm node and an initial hybrid approach is expected. Thus, the most critical layers are printed by EUV technology while other less critical layers are continued with DUV technology. Assuming an EUV introduction in 2018, the ITRS roadmap [2] specifies tight mask registration and overlay specs of 2.2 nm and 3.7 nm, respectively. This requires precise and high-resolution registration metrology not only on DUV masks, but also on patterned high-end EUV reticles.

Given the high absorption of the blank materials at the illumination wavelength of 13.5 nm, EUV technology operates in reflection mode. The reflective multilayer consists of a standard molybdenium silicide (MoSi)-multilayer from Hoya. The absorber was a TaBO/TaBN with a Ruthenium capping layer. The full-spec EUV mask analyzed in this work was written by an high-end variable shaped beam mask writing tool (EBM-9000, Nuflare).

High resolution metrology is a stringent necessity in order to be able to resolve the EUV relevant features of interest and subsequently tune the e-beam writers to achieve the required registration and overlay specifications. In order to achieve the best resolution currently available, we employed a new generation registration tool, the PROVE® HR. Its industry-proven best registration performance originates from the unique combination of its litho-grade optics with a high NA of 0.8, the illumination wavelength of 193 nm and the superior stage concept with tight environment control. The measurement capabilities extend from standard overlay marks to challenging In-die features not only on standard DUV masks, but also on EUV masks as we will show in the following.

Approaching ever smaller nodes with tightening overlay specs, the mask industry experiences a shift to measure more complex features than large overlay crosses. The latter has been measured for decades with a threshold method where the edges of a line profile are determined with high precision. However, threshold evaluation is limited in its use when measuring for example arbitrary shaped features. This applies for example to product-related features, i.e. complex logic patterns, or small features such as very dense contact arrays, which are best suited to calibrate the deflection fields of the latest e-beam writers. To measure such features a more robust and convenient method is to use correlation methods, which take the entire image information into account, i.e. all pixels within a certain region of interest (ROI) [3]. Furthermore, this abrogates potential errors when a threshold profile is coincidentally analyzed at a border of multiple e-beam shots. The key idea of correlation measurements is to determine a registration shift via a correlation of the measured image to a certain reference. The PROVE tool offers three different correlation methods which use different references for the correlation, namely i) Symmetry mode, ii) Database simulation method and iii) Reference image mode.

The Symmetry mode works for symmetric features where an image correlation is performed with the mirrored image of the measured image. For truly arbitrary features the method of choice is the Database simulation, where the reference image originates from a sophisticated aerial image simulation of the given design file. Alternatively, an approach similar to a “Die-to-Die” inspection mode can be employed where the feature of interest has been measured previously on the tool directly and is stored subsequently in a reference database. For all three correlation methods a so-called keyhole functionality can be used, so that also nested features can be analyzed. Instead of using the entire pixel information of the ROI, arbitrary objects can be selected. Subsequently, the boundary of this feature is automatically determined and only the pixels within that selected area are used for correlative imaging analysis (see Figure 1).

In the following we demonstrate registration performance of the distinct measurement modes on three different features patterned on latest EUV blanks, standard Box-In-Box features and Product-related features such as dense pinhole arrays and bar structures.

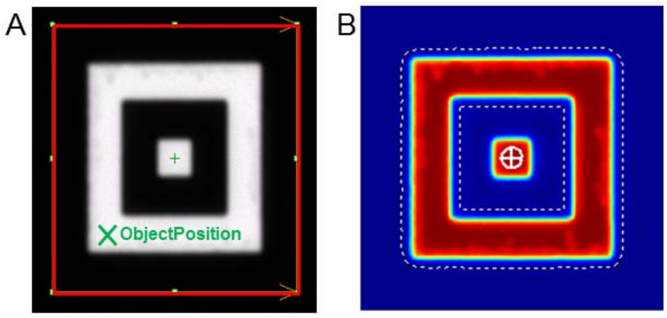

Figure 1: Keyhole functionality for nested objects. Per default all correlation methods take all pixels within the ROI (red rectangle) into account.

A) Nested objects such as the outer frame can be specifically targeted for registration analysis setting an object position (green cross) at the feature of interest within the ROI, here exemplary the outer frame of the Box-In-Box feature.

B) The boundary of the feature is automatically determined (dashed lines in right image) and only pixels within that boundary are used for the image analysis. As a result, the white center cross shows the registration result solely of the outer frame not taking the center contact into account.

STANDARD BOX-IN-BOX FEATURE

In a first step we investigated a standard Box-In-Box feature as shown in Figure 2. Such a standard marker is also processed onto many DUV reticles, hence allowing a comparison of high-end registration performance on EUV masks against current DUV production masks. Given the symmetric design and the feature size with CD≥ 1 µm, all four possible evaluation methods can be applied and compared. In addition, we investigated whether the performance is affected if either the entire Box-In-Box structure or the individual contact in the center is analyzed. As shown in Figure 2B, the repeatability of the individual methods is consistent and stable, particularly for all correlation methods. This also holds for the comparison of the registration of the entire Box-In-Box feature against the individual contact in the center. This clearly indicates that the limited information of the contact only is sufficient for the image analysis to achieve similar repeatability performance. The slightly elevated repeatability for the contact measured with Threshold mode is expected and simply caused by the inherently limited edge information of this method. Overall, comparing these EUV results to repeatability measurements of standard marks on DUV masks, we find no significant difference. Thus, the different composition of EUV masks compared to DUV has no significant effect on the metrology performance. In result, registration markers on EUV masks can be measured with similar performance as high-end DUV masks on the PROVE® HR.

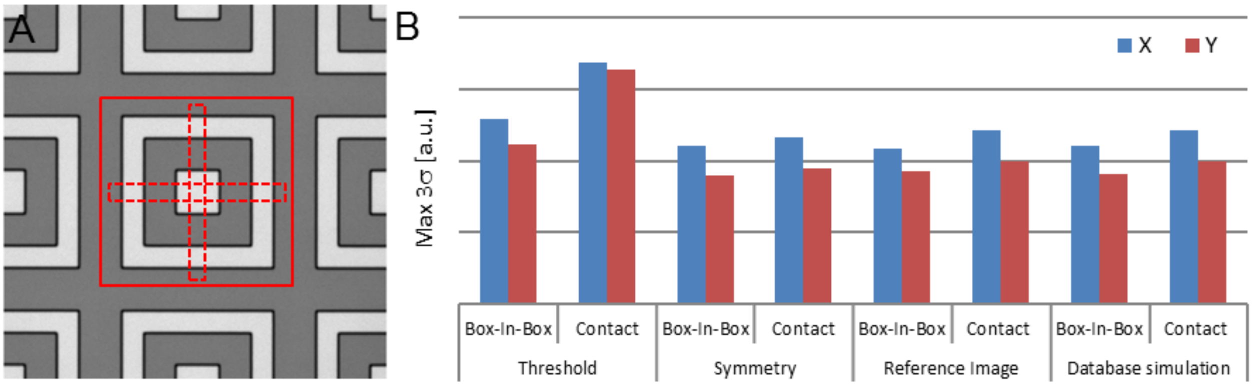

Figure 2: Measurement setup and repeatability performance of a standard Box-In-Box feature on a EUV mask.

A) Box-In-Box feature (CD_{Frame}= 1 µm, $CD_{Contact}$= 2 µm) with an exemplary ROI for the threshold method (dashed red rectangles) and a correlation ROI for entire Box-In-Box (red rectangle) feature as well as the individual contact in the center which was measured using the keyhole functionality.

B) Repeatability performance of standard Box-In-Box feature and individual contact for various measurement modes. Short-term repeatability was determined by measuring 20 loops on a 13x13 grid.

In a next step we investigated the e-beam writing performance across the quality area of the entire mask. As shown in Figure 3, registration after first order compensation shows good results where registration is consistent for the different measurement modes and features. The registration performance on full–spec EUV masks currently accessible by standard metrology is therefore comparable to state of the art DUV masks used for multi-patterning schemes. Recent, yet not published results from comprehensive multi–beam evaluations may indicate that similar performance levels can be expected. However, with EUV lithography the shrink in minimum feature sizes at mask level starts again and mask writing tools have to prove that they are able to achieve the required pattern placement at all mask locations, independent of pattern density, feature type and size.

In order to get there, sophisticated calibration strategies for writing tools are currently under investigation. Therefore a new experimental setup is proposed and explained in detail in the following section.

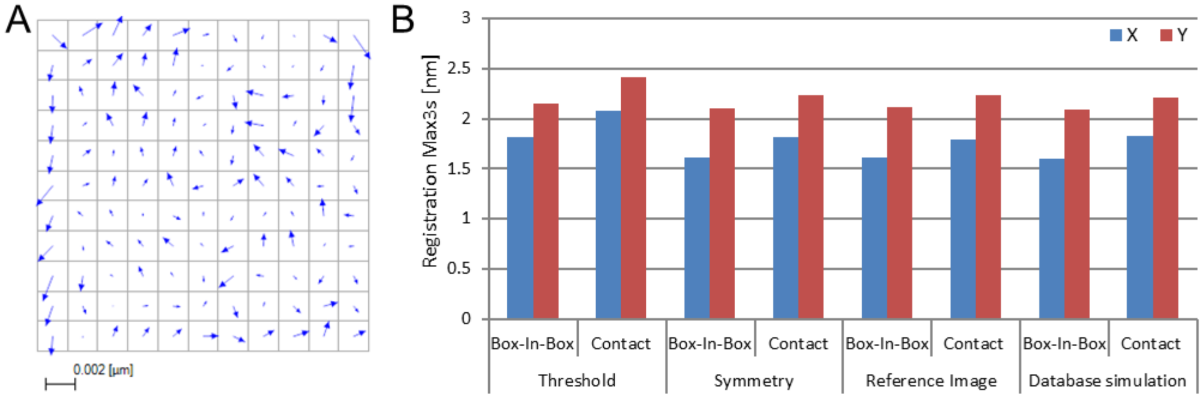

Figure 3: Registration performance.

A) Writing performance of the Box-In-Box structure over the quality area of the EUV mask after first order compensation.

B) Individual registration results for varying measurement modes and features.

E-BEAM CALIBRATION PATTERN

In the following experiment we investigated challenging e-beam calibration structures where a high-resolution metrology tool is of crucial importance to resolve the features of interest. In a first step we evaluated a dense contact array as illustrated in Figure 4, the asymmetric contacts were written with a CD < 120 nm and gaps smaller than 80 nm resulting in a dense duty cycle of about 1.5:1. The excellent resolving power of the registration metrology tool used can be seen in Figure 4D-E where each individual contact is well resolved while the intensity profile exhibits excellent image contrasts up to 46%.-

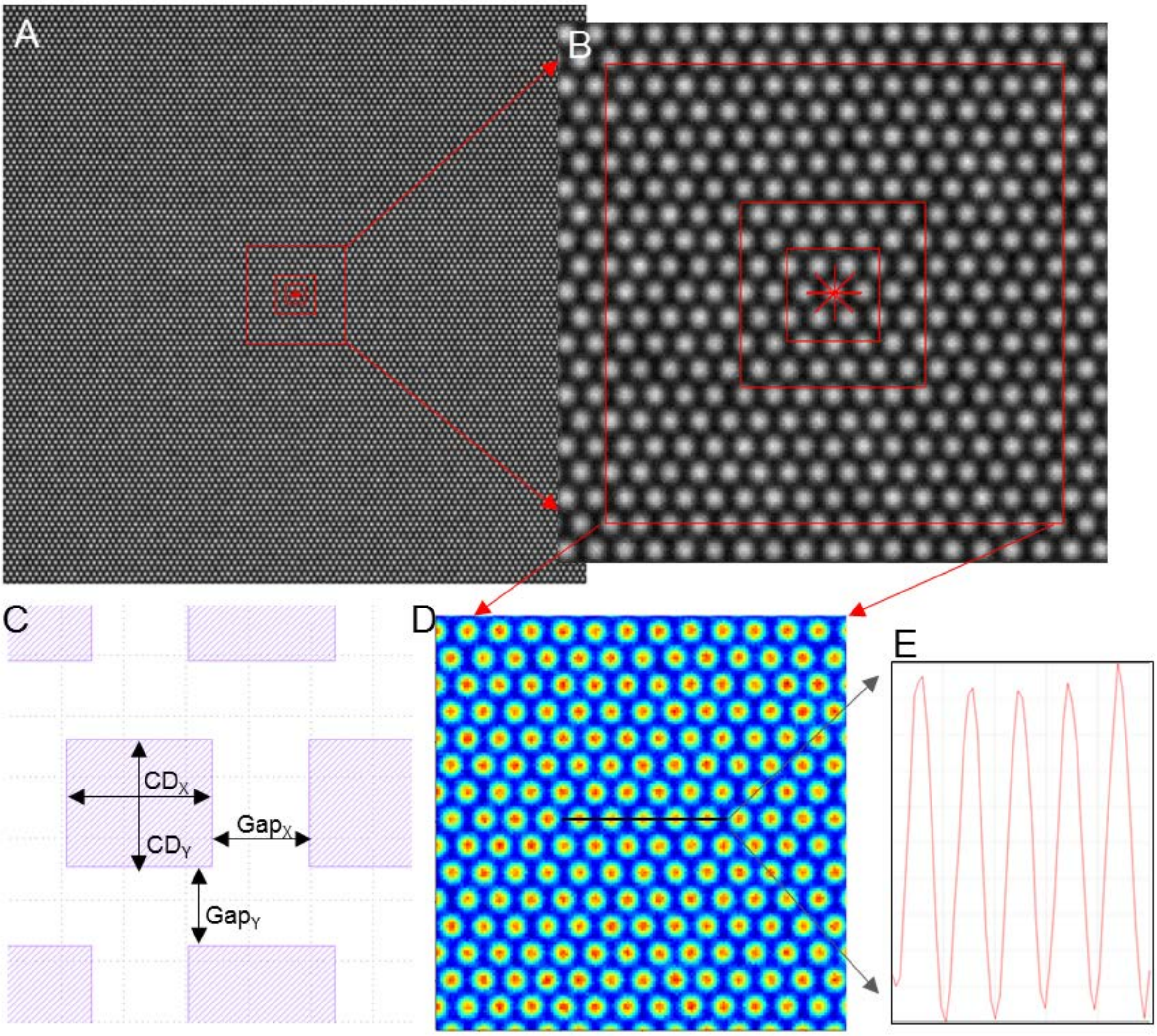

Figure 4: Dense Contact array.

A) Full field-of-view and B) Zoom-In with three different ROI sizes (0.6, 1.2 and 3µm).

C) Design dimensions of the pinhole array varied between 128 sites across the mask and within the rows of the contact array (max. design variation of 3nm). Average values were CD_X=116nm, CD_Y=102nm, Gap_X=78nm, Gap_Y=66 nm.

D) False-color image of dense pinhole array and data (black line) used for intensity profile shown in E). Achieved image contrast was 46%.

Given the asymmetric nature of the contact array, we evaluated the tool performance using the correlation mode with the Database simulation as well as the Reference image. Furthermore, we varied ROI sizes from 0.6 to 3 µm (see Figure 4A/B) taking into account 7, 39 and 255 full contacts for the image analysis, respectively. As shown in Figure 5, the repeatability deteriorates slightly for the smallest ROI as less information is contained in the ROI, but there is no significant increase in the repeatability highlighting a robust registration metrology even for such challenging dense contact arrays. In analogy to the detailed analysis of the different measurement methods for the Box-In-Box feature we also checked the performance of the Database simulation method against the correlation using an acquired reference image. As illustrated in Figure 5 no difference between the measurement modes is visible emphasizing the robustness of the Database simulation.

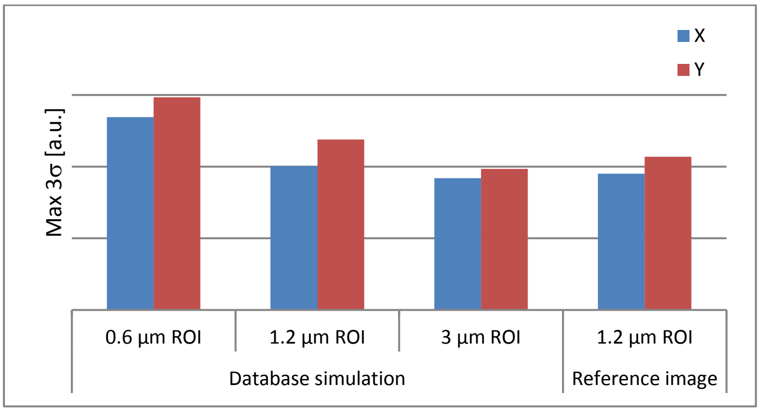

Figure 5: Repeatability of dense contact array for varying ROI sizes and correlation measurement methods (128 sites across the mask area, 10 loops).

In a second step we tested the registration performance of individual contacts on the EUV mask. Given the litho-grade optics of all PROVE systems [4], features can also be measured off-centered from the Field-of-View (FOV). The experimental setup was as follows. A single image stack of the entire FOV was acquired and multiple contacts were individually targeted for registration analysis using the keyhole functionality combined with a database simulation as shown in Figure 6A/B. The advantage of this approach is essentially throughput. Since the stage/mask movement as well as database simulation is required only once, the only time-constraint is the image analysis of these individual contacts. In addition to the remarkable gain in throughput, the instrumental repeatability can be improved as well since the stage repeatability does not contribute statistically. As can be observed from Figure 5C, a clear pattern placement signature is notable then. For further corrections of the writing process such measurable and systematic signatures can be used as feedback to the writing tool.

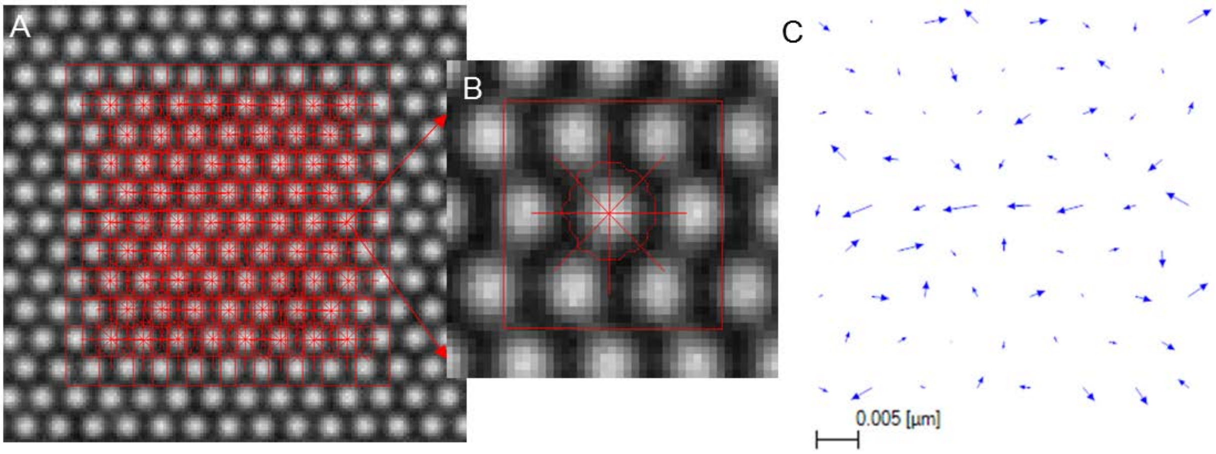

Figure 6: Registration analysis of individual contacts via Keyhole correlation functionality.

A) 68 individual contacts were evaluated out of a dense pinhole array. Only one image stack was acquired while registration of each individual contact was calculated in a multi-measurement fashion applying the keyhole functionality.

B) A correlation boundary (red boundary surrounding the pinhole) is automatically determined within the specified ROI (red rectangle) to identify individual contacts. Subsequently, the precise registration position of a single contact (red cross) is derived from a correlation measurement using only the pixel information within the determined boundary.

C) Registration result after first order compensation.

In the last part we investigated another feature, a bar array with varying CDs (105-160 nm) and gap sizes (30-113 nm) as shown in Figure 7A. With respect to repeatability we analyzed the single bar structure centered in the array via the Database simulation method. Apart from site #4 all 7 features investigated exhibited an excellent repeatability down to lowest CD of 105 nm.

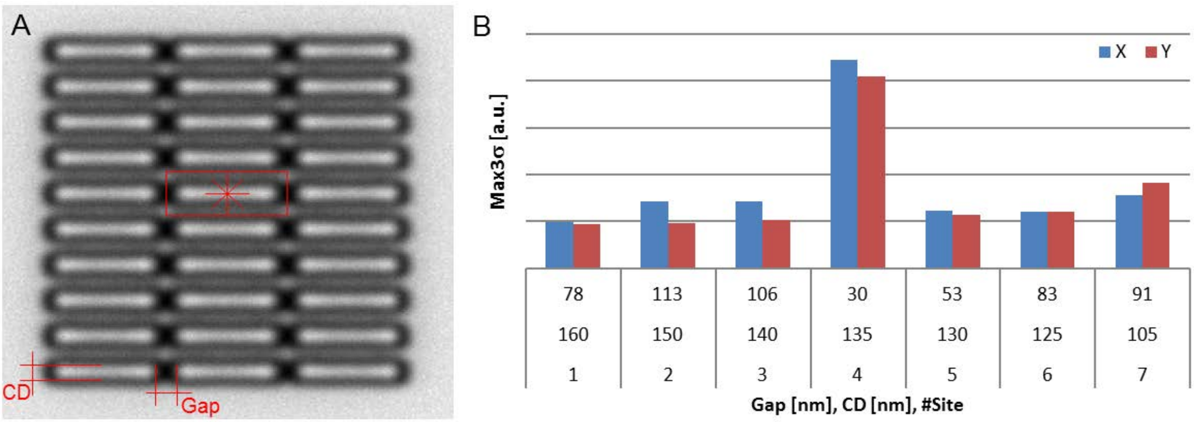

Figure 7: Registration repeatability performance of bar structures.

A) The registration of a single bar structure (red rectangle) was determined via correlation to Database simulation for various combinations of CD and Gap.

B) Repeatability of the individual sites for 20 loops measured.

The significantly higher repeatability of site #4 caught our attention and we started a detailed analysis. In the end, complementary CD-SEM measurements revealed process limitation at the EUV mask itself as the root cause. While the CD of the bars is not the limiting factor, bridging at small gaps sizes such as 30 nm can occur. As exemplary shown in Figure 8, 23 out of 24 tip-to-tip structures exhibit bridging limitations at site #4, thus also limiting the repeatability of the registration results. In a next step we investigated whether the high resolution power of the PROVE® HR allows a qualitative evaluation of these process limitations. The bridging is expected to affect the optical contrast of a line scan across the tip-to-tip feature. This can clearly be observed as demonstrated in Figure 8B. Furthermore, a strong correlation ($R^2 = 0.96$) is seen when comparing the optical contrast against the degree of the process limitation, in this case the effective height of the bridging measured with CD-SEM. Overall we see an excellent matching of optical images between PROVE® HR and CD-SEM data.

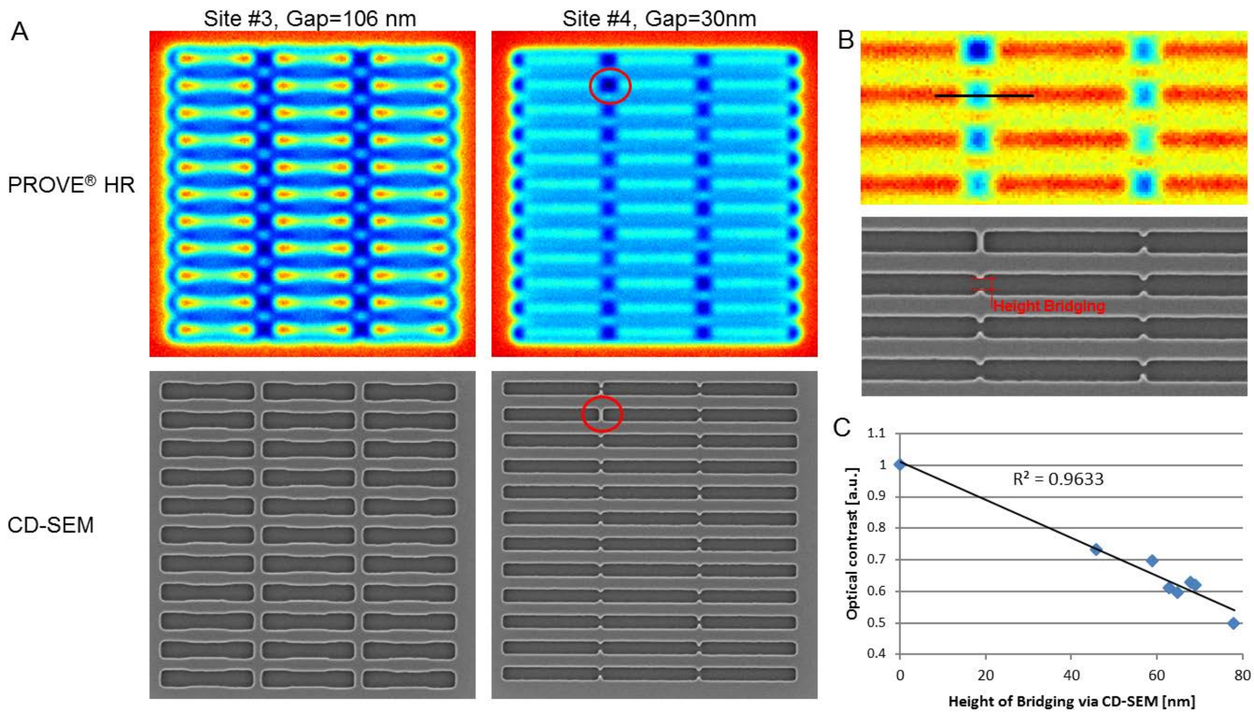

Figure 8: Comparison of PROVE® HR images against SEM data.

A) Both exemplary sites show excellent agreement of PROVE and SEM images. Processing issues, i.e. bridging visible at site #4 with a small nominal gap of only 30 nm, can even qualitatively be evaluated using the high resolution optics of the PROVE® HR.

B) Zoom-in of optical PROVE® HR image and CD-SEM data into Site#4 for with upper left gap corresponding to highlighted gap (red circles) in Figure A.

C) The eight gaps shown in B) were analyzed regarding the optical contrast of the line profile $((I_{max}-I_{min})/(I_{max}+I_{min}))$ including the nominal gap (exemplary black line shown in B) and the height of the bridging determined via CD-SEM. A linear correlation is observed with a $R^2 = 0.96$.

SUMMARY AND CONCLUSIONS

The transition to EUV lithography is now setting another milestone for mask image placement as well as registration metrology. Independent of the writing schemes applied, the mask writing tools have to deal again with shrinking CDs and tighter image placement specifications. In order to support that roadmap new calibration strategies together with sophisticated process technologies have to be developed.

Our investigations demonstrate that suitable high-resolution metrology is already available enabling sophisticated writing tool investigations by matching resolution as well as repeatability requirements at the same time. The high sensitivity of the litho-grade imaging system makes it even possible to detect process limitations which are particularly important in the early phase of process development. Throughput requirements can be met by multi-measurements over the entire field of view of the instrument. In this application a well corrected optical beam path with low aberrations is crucial.

In summary, it becomes clear that high-end registration metrology is dependent on optical resolution power and image contrast. We have shown that further increasing optical resolution and system stability generates an inherent benefit for driving the e-beam performance. This is a key necessity for addressing the challenges introduced by the growing application of EUV lithography for chip manufacturing.

ACKNOWLEDGEMENTS

The authors appreciate the support from the Samsung Mask Development Team for providing the EUV mask under test and the valuable contribution of Dirk Seidel and Susanne Töpfer at ZEISS.

REFERENCES

* contact: Steffen Steinert, steffen.steinert@zeiss.com; phone +49 3641 64-1780; fax +49 3641 64-2938

[1] Z.J. Qi, E. Narita, M. Kagawa, 2015, “Viability of pattern shift for defect-free EUV photomasks at the 7 nm node”, Proc. SPIE 9635, 96350N.

[2] http://www.itrs2.net/2013-itrs.html

[3] D. Seidel, M. Arnz, D. Beyer, 2011, “In-die photomask registration and overlay metrology with PROVE® using 2D correlation methods”, Proc. SPIE 8166, 81661E.

[4] D. Beyer, D. Seidel, S. Heisig, S. Steinert, S. Töpfer, T. Scherübl, J. Hetzler, 2015, "In-die mask registration metrology and the impact of high resolution and low aberrations", Proc. SPIE 9235, 92351S.